Research Article

Effect of sandblasting on the surface roughness and residual stress of 3Y-TZP (zirconia)

Christin Finger[1] · Meike Stiesch[1] · Michael Eisenburger[1] · Bernd Breidenstein[2] · Sarah Busemann[2] · Andreas Greuling[1] (ORCID)

Abstract

A defined surface roughness is important for the adhesive bonding of veneering ceramic to zirconia frameworks. Thus, we investigated the effects that sandblasting has upon the surface roughness and residual stress of zirconia. So as to achieve well-defined blasting parameters and also generate highly reproducible results; a custom-made, automated sandblasting machine was constructed (based on a 3D-printer construction kit). Thirty-two samples (measuring 30 mm × 35 mm × 0.2 mm) were cut from densely sintered 3Y-TZP blanks and then ground with a 45 µm grinding disc. After undergoing regeneration firing, the samples were sandblasted with varying working parameters: blasting angle (45°, 60° and 90°); blasting pressure (2 bar, 4 bar and 6 bar); and working distance (0.5 cm, 1.0 cm and 1.5 cm). The sandblasting path was chosen so as to create samples with an even surface roughness. Changes in blasting pressure resulted in the greatest changes in the surface roughness, the highest surface roughness values were achieved with sandblastings perpendicular to the sample surface. Furthermore, a correlation was found between the mean surface roughness and the residual stress.

1 Introduction

Yttria-stabilized tetragonal zirconia polycrystalline ceramic (Y-TZP), often called zirconia, is a widely used ceramic material for artificial joints, dental implants and implant-abutments, dental crowns and bridges [1, 2]. The white or tooth-coloured zirconia is aesthetically far superior to metal alloys, especially when frameworks of crowns and bridges are exposed. Zirconia implant abutments in the anterior region have the advantage that they do not cause the grey discolouration of thin gingival tissue often observed when metal abutments are used. Moreover, there has been an increasing number of allergies and intolerances observed secondary to the use of dental alloys

over the years [3–5]. In the context of this, the release of metal ions and the effect of their accumulations in lymph nodes and organs has also been a topic of discussion for some time [3, 6]. Zirconia on the contrary is chemically stable, non-toxic and very biocompatible [2, 7–9]. Furthermore, zirconia-based ceramics have a low thermal conductivity and a high mechanical strength, whereas the latter is due to the martensitic phase transformation (tetragonal to monoclinic) which has a key role in transformation toughening [10–14].

It has been shown that a roughening of the surface is useful for various dental applications. A rough ceramic surface improves the osseointegration of ceramic implants and the bonding strength between framework and

✉ Andreas Greuling, greuling.andreas@mh-hannover.de | [1]Department of Prosthetic Dentistry and Biomedical Materials Science, Hannover Medical School, Carl-Neuberg-Straße 1, 30625 Hannover, Germany. [2]Institute of Production Engineering and Machine Tools, Leibniz University Hannover, An der Universität 2, 30823 Garbsen, Germany.

veneering ceramic [15–17]. The improved wettability of the roughened material favours an even blood contact which facilitates osseointegration. With regards to crowns and bridges, the improved wettability of the zirconia-based ceramic supports a better application and firing of the first veneering layer [18, 19]. Nonetheless, no standard procedure has been established for surface roughening in order to achieve the optimal adhesion of veneering ceramic.

Currently, the most common methods used for surface roughening include thermal etching, acid etching, grinding and sandblasting [20]. Factors that need to be taken into consideration for sandblasting include: particle size, exposure time, nozzle size, working distance, blasting pressure and blasting angle [21]. Therefore, the aim of the current study was the development of a sandblasting machine that accounts for all of these factors—in particular allowing a precise adjustment of working distance, blasting pressure and blasting angle—and hence provides a highly reproducible, modifiable sandblasting process for flat zirconia specimens. Moreover, we aimed to examine the effect of the different sandblasting parameters.

2 Materials and methods

2.1 Materials

To evaluate the effects that sandblasting has upon surface and subsurface properties of zirconia, we crafted flat test specimens from 3Y-TZP ceramic blanks (Nacera Pearl 1, Doceram Medical Ceramics GmbH, Germany) (ZrO_2, > 5.5 wt% Y_2O, ≤ 2 wt% HfO_2, < 0.5 wt% Al_2O_3 [22]). After the blanks had been sintered, samples (measuring approximately 30 mm × 35 mm × 0.2 mm) were cut from the blanks with a linear precision saw (Brillant 220, ATM GmbH, Germany). The specimens were then ground in a semi-automatic grinder-polisher unit (PowerPro™ 4000, Buehler, Germany) using a 45 µm diamond grinding disc (Apex DGD 45 µm, 10″, Buehler, Germany) with water cooling. Post-grinding, the samples were cleaned with acetone in an ultrasonic bath for five minutes. Subsequently, a regeneration firing was conducted in a muffle furnace (P310, Nabertherm GmbH, Germany)—in accordance with the VITA Zahnfabrik, Germany, firing parameters [23]—to reverse any possible phase transformations that may have occurred on the surface during the cutting and grinding process. Starting at room temperature (28 °C), the temperature in the furnace was initially raised to 500 °C in 8 min, then heated with a heat-up rate of 100 °C/min to 1000 °C, and fired at 1000 °C for 15 min. After the firing process, the samples were allowed to cool down to room temperature (4.5 h) prior to re-opening the furnace.

32 samples were prepared for the main investigation, with four samples being used for each of eight parameter combinations. The parameter combinations were selected from a preliminary experiment, which is not shown in this manuscript for clarity.

2.2 Sandblasting machine

The machine was based on a 3D-printer construction kit (Reptile, Locxess, Germany), which allows for precisely controlled movements in both the x and y-axes with the help of stepping motors and toothed belts (Fig. 1a). Separate baseplates were mounted onto each of the x-axis and y-axis transfer wagons. The y-axis baseplate had a seated, perforated sample tray affixed to it, and was connected via a funnel and a tube to a suction machine (providing suction in the direction of the blasting). The frame for the perforated sample tray was covered by a sliding lid, which had an opening for the blasting protection tube (Fig. 1b). The x-axis baseplate was equipped with a blasting stylus holder in a pivoting mounting (settable to angles of 45°, 60° and 90°) (Fig. 1c), which was interfaced with one of the three blasting protection tubes (machined to their respective blasting angle) (Fig. 1a). Additional components included in the construction were: a control unit, a sandblaster with pressure regulator (IP Mikro-Sandy, SpezialDental, Germany) and blasting stylus with nozzle (diameter of 1.0 mm for 80–110 µm particle size). The sandblasting machine was operated via a computer installed with the firmware "Marlin" and the control software "Repetier Host" (both supplied with the 3D-printer set). G-Code was used to program the sandblasting movement path into the controller.

2.3 Sandblasting parameters

Prior to setting the various blasting parameters, the samples were fixed with double-sided tape into position onto the perforated sample tray. The blasting angle α was varied via the blasting stylus holder, which could pivot to three different positions (45°, 60° and 90°) with an accuracy of ± 0.25°. The working distance d (between the nozzle and the surface of the zirconia sample) was adjusted by placing spacers—manufactured specifically for the three chosen angles—on top of the specimens (Fig. 2a) and then aligning the blasting stylus holder to the spacer and fixing it into this position. The blasting pressure p was controlled and set manually by the pressure regulator (accuracy of ± 0.2 bar). 110 µm grain alumina (Al_2O_3) (SHERA, Germany) particles were used for the sandblasting process, and the forward blasting speed was set at 3.5 mm/s.

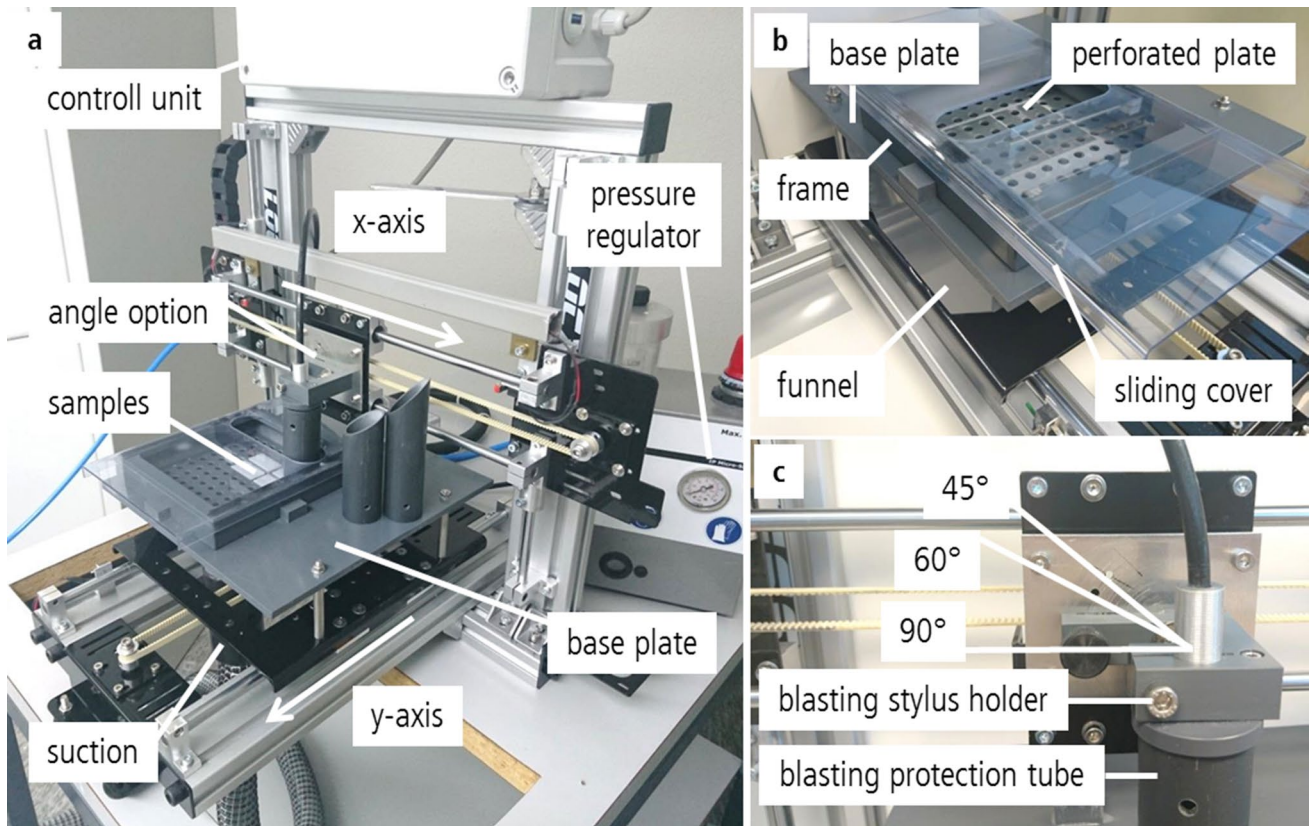Based upon a blasting line width of approximately 1.4 mm (at a distance of 1.0 cm to the sample

Fig. 1 Custom-built automated sandblasting machine (**a**), with y-axis baseplate component details (**b**) and adjustable blasting angle set-up (**c**)

Fig. 2 Adjustment of the working distance using individual spacers for each angle (**a**), sandblasting path with parallel blasting lines 1 mm apart and the profilometry path was perpendicular to the sandblasting path (**b**)
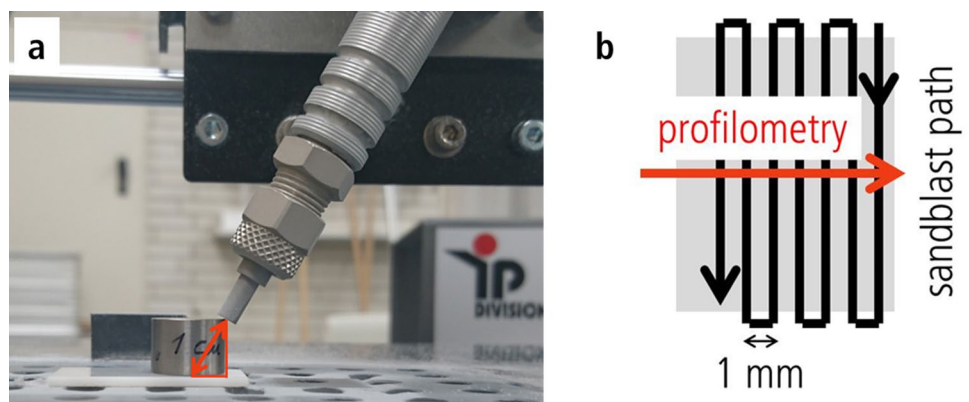
surface—determined during preliminary tests), the distance between the parallel blasting lines was fixed at 1.0 mm to assure that there was overlapping of the sandblasting lines (Fig. 2b).

2.4 Surface roughness measurement

In this study, the arithmetic mean roughness (R_a) was used to assess how evenly distributed the roughening process was, and the mean roughness depth (R_z)

was used as the measure for surface roughness. Both were calculated from profilometry measurements taken perpendicularly to the sandblasting path by a tactile profilometer (Perthometer Concept, Mahr, Germany) (Fig. 2b). For the calculation of the mean roughness depth, each sample underwent profilometry along five separate scanlines, and each of these scanlines were in turn subdivided into five equal parts (0.8 mm long) for analysis—in accordance with DIN EN ISO 4288 [24]. The resulting 25 values (five scanlines each divided into five

segments) were then used to calculate the mean value (R_z) for that sample.

2.5 Residual stress determination

The residual stress was determined for the 32 samples mentioned in 2.1. The residual stress was determined from measurements taken in the middle of each specimen´s treated surface with a diffractometer (XRD 3003 ETA, GE Inspection Technologies Systems GmbH, Germany) by applying the $\sin^2\psi$-method [25]. Measurements were made parallel to the sandblasting path with a 2 mm collimator, Co Kα-radiation with 30 kV and 40 mA, and had a maximum penetration depth of $\tau = 3.1$ µm.

The radiographic method uses the effect of diffraction of X-rays at the crystalline lattice. For this it is necessary to work with monochromatic (Kα1) or at least with quasi-monochromatic X-rays (Kα1 + Kα2). If possible, a single standing peak in the diffractogram, not overlaid by other X-ray reflections, is selected for examination. The position of this peak is in the so-called reflection range, i.e. at a diffraction angle of $2\theta > 90°$. The strains of the crystal lattice deformed by residual stresses are expressed in a displacement of the peak position with respect to the unstrained lattice [26].

2.6 Statistical analysis

A one-way analysis of variances (ANOVA) and Tukey´s pairwise multiple comparisons were used for data analysis. Results are displayed in the form of mean values with standard deviations for each parameter combination, and were considered statistically significant when $p < 0.05$. Furthermore, a three-way ANOVA was performed using distance, pressure and angle as independent variables and Rz and s as dependent variables.

3 Results

With our sandblasting design (in particular the chosen 1 mm distance between blasting lines with a forward blasting speed of 3.5 mm/s) an evenly distributed surface roughening was found irrespective of which parameter combination had been used. An example of this is shown in Fig. 3 for the parameter combination of: working distance 1.0 cm, 6 bar blasting pressure and 90° blasting angle.

32 samples were prepared and sandblasted with the selected eight parameter-combinations (four samples per blasting parameter group). Figure 4 shows the mean surface roughness R_z and mean residual stress of these eight groups.

Specimens from group D exhibited both the highest surface roughness ($R_z = 7.14$ µm ± 0.19 µm) and highest residual stress (s = -1291 MPa ± 19 MPa). Samples in group A had the lowest surface roughness ($R_z = 3.68$ µm ± 0.17 µm). Whereas the lowest residual stress (s = -373 MPa ± 47 MPa) was found in group G. Analysis of variance showed statistically significant differences between all groups ($p < 0.05$). No significant difference was found between the four groups which were sandblasted with 2 bar blasting pressure, but they were all significantly different from the groups sandblasted with 6 bar blasting pressure. Group F and group H were significantly different ($p < 0.05$) from group D and group B significantly different from group H. Furthermore, a 2-side Pearson correlation test for R_z and s was calculated. R_z and s are correlated on a significance level of 0.01.

The Three-way ANOVA for the residual stress s showed the pressure to have the highest non-combined effect (F = 1007, $p < 0.01$), followed by the angle (F = 233, $p < 0.01$) and the distance (F = 13, $p < 0.01$). The highest combined effect was angle*pressure (F = 60, $p < 0.01$), then angle*distance (F = 27, $p < 0.01$) and distance*pressure (F = 11, $p < 0.01$). The test for the combined effect of all three parameters showed no significant result ($p > 0.05$).

Fig. 3 Profilometry for a sample sandblasted with a working distance of 1.0 cm, blasting pressure of 6 bar, 90° blasting angle and a forward speed of 3.5 mm/s
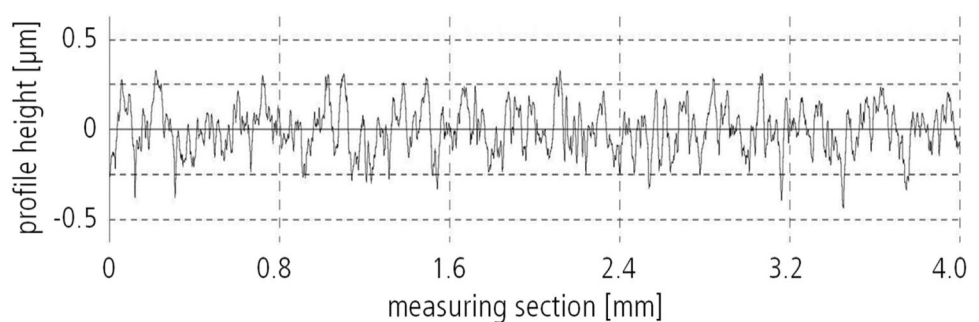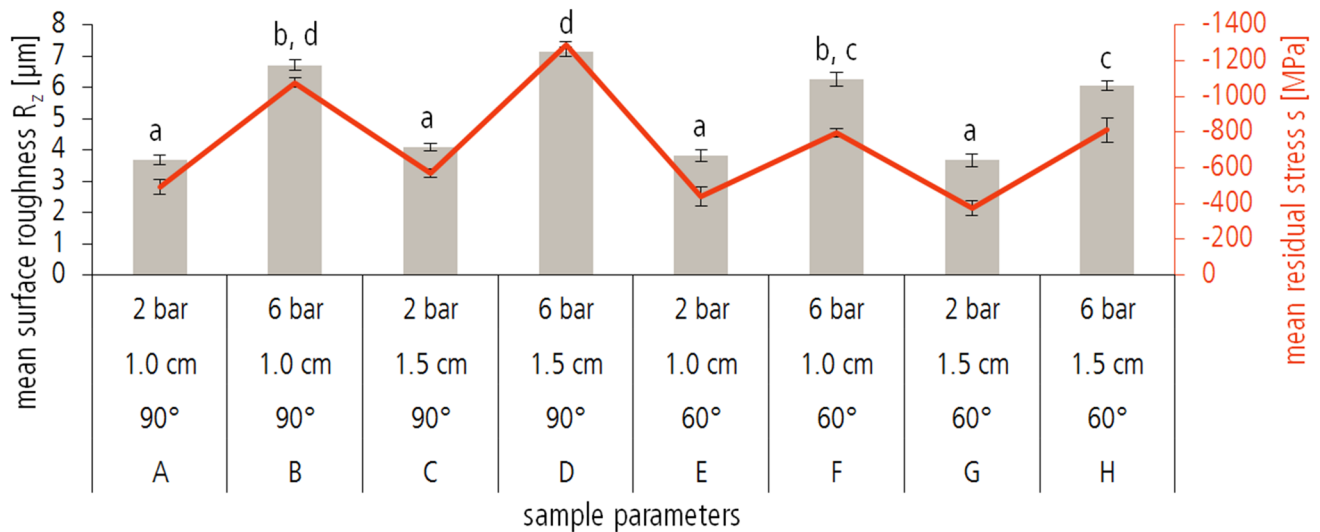
Fig.4 Mean surface roughness R_z and mean residual stress post-sandblasting with selected parameter combinations for lowest and highest surface roughness (with standard deviation), identical lower-case letters indicate groups with non-significant differences ($p > 0.05$) between their mean R_z values. Without sandblasting the surface roughness R_z was 0.12 µm ± 0.01 µm and the residual stress s was -18 MPa ± 2 MPa

The Three-way ANOVA for the mean surface roughness R_z showed the highest effect for pressure (F = 1491, $p < 0.01$), then angle (F = 41, $p < 0.01$), angle*pressure (F = 20, $p < 0.01$) and angle*distance (F = 17, $p < 0.01$). The Distance and the other combined effects showed no significant result ($p > 0.05$).

For the ease of comparison with other studies, Fig. 5 presents both the mean roughness R_a and the mean roughness depth R_z (mean values and standard deviations) with their associated selected working parameters.
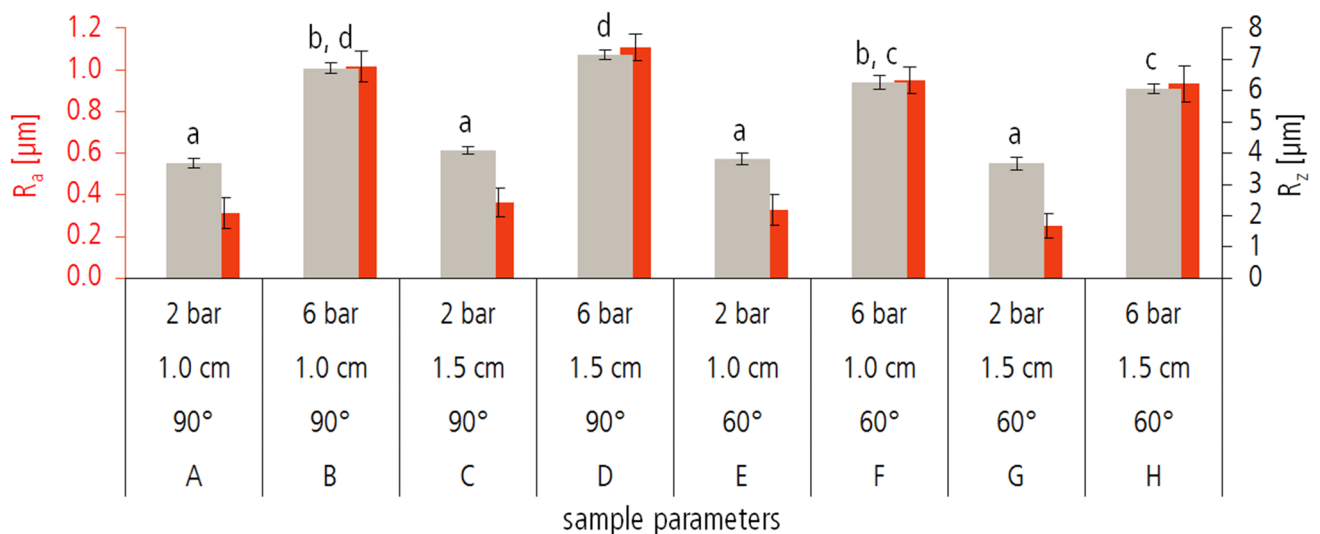
The highest R_a-value were found in group D ($R_a = 1.11$ µm ± 0.06 µm), and the lowest in group G. All results for mean surface roughness R_z and R_a and mean residual stress s with standard deviation are summarised in Table 1.

Fig. 5 Mean surface roughness R_a and R_z of selected parameter combinations used to generate lowest and highest surface roughness values (with standard deviation), identical lower-case letters indicate groups with non-significant differences (p > 0.05) between their mean values. Without sandblasting the surface roughness values were $R_a = 0.01$ µm ± 0.00 µm and $R_z = 0.12$ µm ± 0.01 µm

Table 1 Summary of mean surface roughness (R_z and R_a) and mean residual stress (s) with standard deviation

Group	Blasting angle α [°]	Working distance d [cm]	Blasting pressure p [bar]	R_z [μm]	R_a [μm]	s [MPa]
A	90	1.0	2	3.68 ± 0.17	0.31 ± 0.08	− 492 ± 49
B			6	6.71 ± 0.19	1.02 ± 0.08	− 1077 ± 32
C		1.5	2	4.08 ± 0.15	0.36 ± 0.07	− 570 ± 30
D			6	7.14 ± 0.19	1.11 ± 0.06	− 1291 ± 19
E	60	1.0	2	3.81 ± 0.21	0.33 ± 0.08	− 440 ± 59
F			6	6.25 ± 0.26	0.95 ± 0.06	− 796 ± 30
G		1.5	2	3.68 ± 0.23	0.25 ± 0.06	− 373 ± 47
H			6	6.06 ± 0.18	0.93 ± 0.09	− 812 ± 79
Without sand-blasting				0.12 ± 0.01	0.01 ± 0.00	− 18 ± 2

4 Discussion

The degree of surface roughness is important for zirconia frameworks, enhancing their wettability and micromechanical interlocking to the veneering ceramic [19, 27]. Sandblasting, grinding, and acid or thermal etching (or combinations of these) are some of the more commonly used methods for surface roughening [20, 27]. Moreover, sandblasting of 3Y-TZP surfaces causes phase transformations from the metastable tetragonal phase to the monoclinic phase [1]. Phase transformations were examined in several studies with X-ray diffraction, where the content of monoclinic phase increased after sandblasting [21, 28–30]. These phase transformations result in compressive stress in the surface layers. The compressive stress can counteract tensile stress which might occur under load, thereby increasing the strength of the material in the layers close to the surface [31]. Gentle sandblasting can achieve positive effects such as improved wettability, mechanical interlocking and the above-mentioned compressive stress field in the layers close to the surface. Whereas severe sandblasting might damage the material beyond the transformed region, weakening the zirconia-based material rather than strengthening it. One example for such a case has been reported by Chintapalli et al. [28]. The authors stated that the expectations when sandblasting zirconia with 250 μm alumina particles at 2 bar, would be of a reduction in the material's strength, since the depth of the resulting damage would be much greater than the depth of the compressive residual stress field.

In the current study, samples sandblasted perpendicularly to their surface ($\alpha = 90°$) and 1.5 cm working distance, demonstrated a higher surface roughness than samples sandblasted with a blasting angle of 60° and 1.5 cm working distance. Though, the greatest effects on both surface roughness and residual stress were seen with changes in the blasting pressure. In aid of comparing our study's findings with the literature, an estimated blasting time t was calculated by dividing the width of the blasting area by the forward speed. Table 2 provides a comparative overview of mean roughness values R_a before and after sandblasting from several studies. When comparing our results

Table 2 Parameters and mean roughness R_a before and after sandblasting from a selection of other studies and the present paper (selected parameter combinations for comparison)

Reference	Grain size A_2O_3 [μm]	Distance d [cm]	Time t [s]	Pressure p [bar]	Angle α [°]	Without sandblasting R_a [μm]	With sandblasting R_a [μm]
He et al. [27]	100	1	10	2	N/A	0.63 ± 0.42	0.89 ± 0.35
Abi-Rached et al. [19]	120	1	15	2.8	90	0.35 ± 0.05	0.80 ± 0.04
Nakamura et al. [32]	70	1	10	2	N/A	0.1 or less	0.23 ± 0.10
				6	N/A	0.1 or less	0.30 ± 0.10
Liu et al. [33]	50	1	15	3.5	90	0.196 ± 0.026	1.314 ± 0.138
Current study	110	1	0.4	2	60	0.01 ± 0.00	0.33 ± 0.07
					90	0.01 ± 0.00	0.31 ± 0.07
				6	60	0.01 ± 0.00	0.95 ± 0.06
					90	0.01 ± 0.00	1.02 ± 0.07

with the work of He et al. [27] (2 bar blasting pressure and 1 cm working distance) and Abi-Rached et al. [19] (2.8 bar blasting pressure and 1 cm working distance) their resultant surface roughness proved to be much higher (details given Table 2). This may be related in part to both the surface roughness before sandblasting and the blasting times being greater in both of their studies. Additionally, the blasting angle was not mentioned by He et al. but Abi-Rached et al. did report sandblasting perpendicular to the surface. The results of Nakamura et al. [32] with 70 μm Al_2O_3 and 6 bar blasting pressure corresponded with the surface roughness of samples sandblasted with 110 μm and 2 bar blasting pressure in this paper. The surface roughness values obtained in the current paper from samples sandblasted with 6 bar blasting pressure were three times greater than those from Nakamura et al. In the study of Liu et al. zirconia samples were sandblasted perpendicular to the surface at a pressure of 3.5 bar, with a working distance of 1 cm and a grain size of 50 μm [33]. The surface roughness Liu et al. obtained were higher than the result of the current study for 6 bar and 110 μm grain size. Again, the explanation might lie in the different blasting times, grain size or blasting path.

When comparing the results of surface roughness after sandblasting in the selected studies, no correlations between different blasting parameters and the resulting surface roughness can be found. Passos et al. [34] explained that "air-abrasion was performed by making circular movements with the nozzle" but this can also vary from sample to sample and is dependent on the investigator. These factors can explain the different results from various studies even when the remaining parameters are comparable. For this reason an automated, mobile sandblasting machine was constructed for use in this current study—to eliminate the problems inherent with manual processing. Correspondingly, the resultant surface treatments are all highly reproducible since a computer-controlled sandblasting path was used, in conjunction with the ease of precisely setting the requisite blasting parameters.

The results of the current study show a correlation between surface roughness and residual stress of sandblasted samples. However, other surface treatment methods have shown different results. When grinding a 3Y-TZP ceramic with diamond as the abrasive, with an average grain size of 15 μm or 251 μm, Denkena et al. [35] measured a surface roughness R_z approximately between 2 μm and 25 μm and residual stress approximately between −100 MPa and −900 MPa. The current study showed R_z-values approximately between 3 μm and 7 μm and residual stress between −400 MPa and −1300 MPa. Consequently no direct conclusion can be drawn from the surface roughness to the residual stress. This has to be taken into consideration when surfaces are roughened by sandblasting, as there might be a limit to the observed correlation. Gentle sandblasting can achieve positive effects such as improved wettability and mechanical interlocking, as well as the phase transformation compressive stress field in the surface layers which increases the strength of the zirconia-based material. Severe sandblasting on the contrary, which damages the material beyond the transformed region, could weaken the material.

5 Conclusion

Within the limitations of this study, it was shown that the residual stress correlates with the mean surface roughness R_z after sandblasting. The highest residual stress and surface roughness was found after sandblasting perpendicular to the surface. Among the parameters blasting angle, blasting pressure and working distance, the blasting pressure showed the greatest effect on surface roughness and residual stress with the parameter range tested in this work. Further research is needed to evaluate the effect of these different surface treatment regimens on the adhesive bond strength after veneering with feldspar ceramic.

Complaince with ethical standards

Conflict of interest The author declare that they have no conflict of interest.

References

1. Denry I, Kelly JR (2008) State of the art of zirconia for dental applications. Dent Mater 24:299–307. https://doi.org/10.1016/j.dental.2007.05.007

2. Sivaraman K, Chopra A, Narayan AI, Balakrishnan D (2017) Is zirconia a viable alternative to titanium for oral implant? A critical review. J Prosthodont Res. https://doi.org/10.1016/j.jpor.2017.07.003

3. Agarwal A, Tyagi A, Ahuja A, Kumar N, De N, Bhutani H (2014) Corrosion aspect of dental implants—An overview and literature review. OJST 04:56–60. https://doi.org/10.4236/ojst.2014.42010

4. Chaturvedi T (2013) Allergy related to dental implant and its clinical significance. Clin Cosmet Investig Dent 5:57–61. https://doi.org/10.2147/CCIDE.S35170

5. Syed M, Chopra R, Sachdev V (2015) Allergic reactions to dental materials-a systematic review. J Clin Diagn Res. https://doi.org/10.7860/JCDR/2015/15640.6589

6. Mueller CK, Solcher P, Peisker A, Mtsariashvili M, Schlegel KA, Hildebrand G, Rost J, Liefeith K, Chen J, Schultze-Mosgau S (2013) Analysis of the influence of the macro- and microstructure of dental zirconium implants on osseointegration: a minipig study, Oral Surg Oral Med Oral Pathol Oral Radiol 116:8. https://doi.org/10.1016/j.oooo.2011.10.041

7. Ardlin BI (2002) Transformation-toughened zirconia for dental inlays, crowns and bridges chemical stability and effect of low-temperature aging on flexural strength and surface structure. Dent Mater 18(8):590–595

8. Christel P, Meunier A, Heller M, Torre JP, Peille CN (1989) Mechanical properties and short-term in vivo evaluation of yttria-oxide-partially-stabilized zirconia. J Biomed Mater Res 2:45–61

9. Piconi C, Maccauro G (1999) Zirconia as a ceramic biomaterial. Biomaterials 20:1–25. https://doi.org/10.1016/S0142-9612(98)00010-6

10. Kelly JR, Denry I (2008) Stabilized zirconia as a structural ceramic: an overview. Dent Mater 24:289–298. https://doi.org/10.1016/j.dental.2007.05.005

11. Kelly PM, Francis Rose LR (2002) The martensitic transformation in ceramics—its role in transformation toughening. Prog Mater Sci 47:463–557. https://doi.org/10.1016/S0079-6425(00)00005-0

12. Chevalier J (2006) What future for zirconia as a biomaterial? Biomaterials 27:535–543. https://doi.org/10.1016/j.biomaterials.2005.07.034

13. de Aza AH, Chevalier J, Fantozzi G, Schehl M, Torrecillas R (2002) Crack growth resistance of alumina, zirconia andzirconia toughened alumina ceramics for joint prostheses. Biomaterials 23(3):937–945

14. Guazzato M, Albakry M, Ringer SP, Swain MV (2004) Strength, fracture toughness and microstructure of a selection of all-ceramic materials. Part II. Zirconia-based dental ceramics. Dent Mater. https://doi.org/10.1016/j.dental.2003.05.002

15. Bankoğlu Güngör M, Yılmaz H, Karakoca Nemli S, Turhan Bal B, Aydın C (2015) Effect of surface treatments on the biaxial flexural strength, phase transformation, and surface roughness of bilayered porcelain/zirconia dental ceramics. J Prosthet Dent. https://doi.org/10.1016/j.prosdent.2014.12.002

16. Mendonça G, Mendonça DBS, Aragão FJL, Cooper LF (2008) Advancing dental implant surface technology–from micron-to nanotopography. Biomaterials 29:3822–3835. https://doi.org/10.1016/j.biomaterials.2008.05.012

17. Monaco C, Cardelli P, Scotti R, Valandro LF (2011) Pilot evaluation of four experimental conditioning treatments to improve the bond strength between resin cement and Y-TZP ceramic. J Prosthodont 20:97–100. https://doi.org/10.1111/j.1532-849X.2010.00677.x

18. Rupp F, Gittens RA, Scheideler L, Marmur A, Boyan BD, Schwartz Z, Geis-Gerstorfer J (2014) A review on the wettability of dental implant surfaces I: theoretical and experimental aspects. Acta Biomater. https://doi.org/10.1016/j.actbio.2014.02.040

19. Abi-Rached FO, Martins SB, Campos JA, Fonseca RG (2014) Evaluation of roughness, wettability, and morphology of an yttria-stabilized tetragonal zirconia polycrystal ceramic after different airborne-particle abrasion protocols. J Prosthet Dent 112:1385–1391. https://doi.org/10.1016/j.prosdent.2014.07.005

20. Grigore A, Spallek S, Petschelt A, Butz B, Spiecker E, Lohbauer U (2013) Microstructure of veneered zirconia after surface treatments: a TEM study. Dent Mater 29:1098–1107. https://doi.org/10.1016/j.dental.2013.07.022

21. Guazzato M, Quach L, Albakry M, Swain MV (2005) Influence of surface and heat treatments on the flexural strength of Y-TZP dental ceramic. J Dent 33:9–18. https://doi.org/10.1016/j.jdent.2004.07.001

22. DOCERAM Medical ceramics GmbH, technical data: chemical composition (2017) https://nacera.de/en/products-solutions/zirconia-products/nacera-pearl-1/

23. VITA Zahnfabrik, VITA YZ T/ VITA YZ HT: Working instructions (2016)

24. Mahr GmbH, Selection of cutoff: EN ISO 4288, ASME B46.1. https://www.mahr.com/Mahr-Parameter/html/english/MarSurf/grenzwellenlaenge.html

25. Macherauch E, Mueller P (1961) Das $\sin^2\psi$-Verfahren der roentgenographischen Spannungsmessung. Zeitschrift für angewandte Physik 13(7):305–312

26. Breidenstein B (2011) Oberflaechen und Randzonen hoch belasteter Bauteile. Produktionstechn. Zentrum, PZH

27. He M, Zhang Z, Zheng D, Ding N, Liu Y (2014) Effect of sandblasting on surface roughness of zirconia-based ceramics and shear bond strength of veneering porcelain. Dent Mater J 33:778–785. https://doi.org/10.4012/dmj.2014-002

28. Chintapalli RK, Marro FG, Jimenez-Pique E, Anglada M (2013) Phase transformation and subsurface damage in 3Y-TZP after sandblasting. Dent Mater. https://doi.org/10.1016/j.dental.2013.03.005

29. KosmacOblakJevnikarFundukMarion TCPNL (1999) The effect of surface grinding and sandblasting on flexural strength and reliability of Y-TZP zirconia ceramic. Dent Mater 15(6):426–433

30. Sato H, Yamada K, Pezzotti G, Nawa M, Ban S (2008) Mechanical properties of dental zirconia ceramics changed with sandblasting and heat treatment. Dent Mater J 27:408–414

31. Guazzato M, Albakry M, Quach L, Swain MV (2004) Influence of grinding, sandblasting, polishing and heat treatment on the flexural strength of a glass-infiltrated alumina-reinforced dental ceramic. Biomaterials. https://doi.org/10.1016/j.biomaterials.2003.08.056

32. Nakamura T, Wakabayashi K, Zaima C, Nishida H, Kinuta S, Yatani H (2009) Tensile bond strength between tooth-colored porcelain and sandblasted zirconia framework. J Prosthodont Res 53:116–119. https://doi.org/10.1016/j.jpor.2009.02.007

33. Liu D, Matinlinna JP, Tsoi JK-H, Pow EHN, Miyazaki T, Shibata Y, Kan C-W (2013) A new modified laser pretreatment for porcelain zirconia bonding. Dent Mater 29:559–565. https://doi.org/10.1016/j.dental.2013.03.002

34. Passos SP, Linke B, Major PW, Nychka JA (2015) The effect of air-abrasion and heat treatmenton the fracture behavior of Y-TZP. Dent Mater 31:1011–1021. https://doi.org/10.1016/j.dental.2015.05.008

35. Denkena B, Breidenstein B, Busemann S, Lehr CM (2017) Impact of hard machining on zirconia based ceramics for dental applications, procedia. CIRP. https://doi.org/10.1016/j.procir.2017.04.055